OPEN

Molecular Profiling of Sinonasal Adenoid Cystic Carcinoma

Canonical and Noncanonical Gene Fusions and Mutation

Alena Skálová, MD, PhD,† Martina Bradová, MD, PhD,*† Abbas Agaimy, MD, PhD,‡ Jan Laco, MD, PhD,§ Cécile Badual, MD, PhD,‖ Stephan Ihrler, MD, PhD,¶ Ivan Damjanov, MD, PhD,# Niels J. Rupp, MD, PhD,** Carlos E. Bacchi, MD,†† Sarina Mueller, MD, PhD,‡‡ Sami Ventelä, MD, PhD,§§ Da Zhang, MD, PhD,‖‖ Eva Comperat, MD, PhD,¶¶## Petr Martínek, PhD,*** Radek Šíma, PhD,**** Tomas Vaněček, PhD,*** Petr Grossmann, PhD,*** Petr Steiner, PhD,*** Veronka Hájková, PhD,*** Inka Kovářová, MD,* Michal Michal, MD,*† and Ilmo Leivo, MD, PhD†††‡‡‡*

Abstract: Adenoid cystic carcinomas (AdCC) of salivary gland origin have long been categorized as fusion-defined carcinomas owing to the almost universal presence of the gene fusion *MYB::NFIB,* or less commonly *MYBL1::NFIB.* Sinonasal AdCC is an aggressive salivary gland malignancy with no effective systemic therapy. Therefore, it is urgent to search for potentially targetable genetic alterations associated with AdCC. We have searched the authors' registries and selected all AdCCs arising in the sinonasal tract. The tumors were examined histologically, immunohistochemically, by next generation sequencing (NGS) and/or fluorescence in situ hybridization (FISH) looking for *MYB*/*MYBL1* and/or *NFIB* gene fusions or any novel gene fusions and/or mutations. In addition, all tumors were tested for HPV by genotyping using (q)PCR. Our cohort comprised 88 cases of sinonasal AdCC, predominantly characterized by canonical *MYB::NFIB* (49 cases) and *MYBL1::NFIB* (9 cases) fusions. In addition, noncanonical fusions *EWSR1::MYB*; *ACTB::MYB; ESRRG::DNM3,* and *ACTN4::MYB* were identified by NGS, each of them in 1 case. Among nine fusion-negative AdCCs, FISH detected rearrangements in *MYB* (7 cases)*, NFIB* (1 case), and *EWSR1* (1 case). Six AdCCs lacked fusions or gene rearrangements, while 11 cases were unanalyzable. Mutational analysis was performed by NGS in 31/88 (35%) AdCCs. Mutations in genes with established roles in oncogenesis were identified in 21/31 tumors (68%), including *BCOR* (4/21; 19%),

From the *Department of Pathology, Charles University, Faculty of Medicine in Pilsen; †Bioptic Laboratory Ltd; ***Molecular and Genetic Laboratory, Bioptic Laboratory Ltd, Pilsen; §The Fingerland Department of Pathology, Charles University, Faculty of Medicine and University Hospital Hradec Kralove, Hradec Kralove, Czech Republic; ‡Institute of Pathology, University Hospital Erlangen, Friedrich-Alexander University Erlangen-Nürnberg (FAU); ‡‡Department of Otorhinolaryngology and Head and Neck Surgery, University Hospital Erlangen, Erlanden; ¶Dermpath, Muenchen, Germany; ‖Service d'Anatomo-Pathologie, Department of Pathology, Hôpital Européen G Pompidou, APHP, Université de Paris; ¶¶Department of Pathology, Tenon Hospital, Sorbonne University, Paris, France; #The University of Kansas School of Medicine; ‖‖Department of Pathology and Laboratory Medicine, The University of Kansas Medical Center, Kansas City, KS; **Department of Pathology, and Molecular Pathology, University Hospital Zurich, Zurich, Switzerland; ††Consultoria em Patologia, Botucatu, São Paulo, Brazil; ##Department of Pathology, Medical University of Vienna, Vienna, Austria; Departments of §§Otorhinolaryngology; ‡‡‡Pathology, Turku University Hospital; and †††Institute of Biomedicine, Pathology, University of Turku, Turku, Finland.

The preliminary results of the study were presented as a poster presentation at the United States and Canadian Academy of Pathology's 113th Annual Meeting, March 23 to 28, 2024, in Baltimore, Maryland, USA.

The part of the results of the same cohort have been recently published in *American Journal Surgical Pathology.*

A.S., M.B., M.M., and I.L.: conception and design of the work, acquisition, analysis and interpretation of data, drafting the MS, and revising it critically for important intellectual content and scientific integrity. T.V., R.Š., P.G., P.S., V.H., and P.M.: performance and interpretation of molecular-genetic analysis, revising it critically for important intellectual content and scientific integrity. A.A., J.L., C.B., S.I., E.C., I.D., C.B., I.K., and N.J.R.: providing the case, reading and revising the MS critically for important intellectual content, and scientific integrity. S.M. and S.V.: providing follow-up data, reading and revising the MS critically for important intellectual content, and scientific integrity. All authors have read and approved the final manuscript.

Conflicts of Interest and Source of Funding: This study was supported by study grant SVV 260652 from the Ministry of Education of the Czech Republic (N.K.), the Cooperatio Program—research area SURG from the Charles University, Czech Republic (N.K., M.B., A.S.), the project National Institute for Cancer Research—NICR (Programme EXCELES, ID Project No. LX22NPO5102)—Funded by the European Union—Next Generation EU (A.S. and M.B.), and the Finnish Cancer Society, Finska Läkaresällskapet, the Turku University Hospital Fund, and the Maritza and Reino Salonen Foundation, Finland (I.L.). For the remaining authors none were declared.

Correspondence: Alena Skálová, MD, PhD, Sikl's Department of Pathology, Charles University, Faculty of Medicine in Pilsen, E. Benese 13, Pilsen 305 99, Czech Republic (e-mail: skalova@biopticka.cz).

DOI: 10.1097/PAS.0000000000002349

NOTCH1 (3/21; 14%), *EP300* (3/21; 14%), *SMARCA4* (2/21; 9%), *RUNX1* (2/21; 9%), *KDM6A* (2/21; 9%), *SPEN* (2/21; 9%), and *RIT1, MGA, RB1, PHF6, PTEN, CREBBP, DDX41, CHD2, ROS1, TAF1, CCD1, NF1, PALB2, AVCR1B, ARID1A, PPM1D, LZTR1, GEN1*, *PDGFRA*, each in 1 case (1/21; 5%). Additional 24 cases exhibited a spectrum of gene mutations of uncertain pathogenetic significance. No morphologic differences were observed between AdCCs with *MYBL1::NFIB* and *MYB::NFIB* fusions. Interestingly, mutations in the *NOTCH* genes were seen in connection with both canonical and noncanonical fusions, and often associated with high-grade histology or metatypical phenotype, as well as with poorer clinical outcome. Noncanonical fusions were predominantly observed in metatypical AdCCs. These findings emphasize the value of comprehensive molecular profiling in correlating morphologic characteristics, genetic landscape, and clinical behavior in AdCC.

Key Words: salivary gland neoplasm, sinonasal, adenoid cystic carcinoma, *ACTN4/EWSR1/ACTB::MYB* gene fusion, novel *ESRRG::DNM3* gene fusion, gene *NOTCH* mutation

(*Am J Surg Pathol* 2025;49:227–242)

Adenoid cystic carcinoma (AdCC) is one of the most common salivary carcinomas and occurs in all major and minor salivary gland and seromucous gland sites. AdCC is an invasive malignancy composed of epithelial and myoepithelial neoplastic cells arranged in tubular, cribriform, and solid patterns. It is associated with eosinophilic extracellular matrix and reduplicated basement membrane materials, and often with gene fusions involving the *MYB, MYBL1,* and *NFIB* genes.[1] The genomic hallmarks of AdCC are t(6;9) or t(8;9) translocations, resulting in *MYB:NFIB* and *MYBL1:NFIB* fusions, respectively.[2,3] The former alteration is found in $>80\%$ of the cases and the latter in $\sim 5\%$.[3] *MYB/MYBL1* activation due to gene fusion or other mechanisms is a key event in the pathogenesis of AdCC.[2] Losses of 1p, 6q, and 15q were shown earlier to be associated with high-grade morphology, while loss of 14q is seen exclusively in low-grade tumors.[4,5] Our group published recently a study of a cohort of salivary adenoid cystic carcinomas of major glands and sinonasal minor glands that harbored non-canonical novel fusions *TULP4:MYB, ACTB:MYB, ACTN4:MYB*, and *ESRRG:DNM3*.[6]

AdCC is typically a slow-growing neoplasm with protracted clinical course and poor long-term prognosis.[7,8] Although AdCC rarely metastasizes to regional lymph nodes,[9] local recurrence and distant metastases, most commonly to the lung followed by bone, liver, and brain, are frequent in later stages of the disease.[10,11]

Although sinonasal tumors constitute only a small fraction of head and neck tumors, they encompass a diverse spectrum of epithelial, mesenchymal, and neuroectodermal neoplasms, and their diagnosis and treatment is challenging. Sinonasal AdCC is a highly aggressive salivary gland malignancy without effective systemic therapy. Standard treatment includes surgical resection and postoperative radiotherapy, but the efficacy of postoperative chemotherapy remains unclear, and specific treatment for AdCC has not yet been established. The clinical course for patients with AdCC primarily arising in minor salivary/seromucous glands of nasal cavity and paranasal sinuses is especially unfavorable. Sinonasal AdCC commonly invades locally by destroying adjacent bone and/or through perineural or perivascular spread along the second and third divisions of the trigeminal nerve. Due to usually late presentation and diagnosis, these tumors may invade the orbit and/or exhibit intracranial expansion. While complete surgical resection of AdCC is the treatment of choice,[12] it is often not possible in sinonasal sites, leading to frequent recurrences and often distant metastases.[12]

Given these challenges, it is urgent to search for potentially targetable genetic alterations associated with sinonasal AdCC. Next-generation sequencing of AdCC has identified mutations, mostly with a low level of recurrence, in genes involved in the *FGF/IGF/PI3K*, chromatin remodelling, and *NOTCH* signaling pathways.[13,14] Notably, the presence of *NOTCH* alterations in AdCC has been shown to associate with poor survival.[15] Ferrarotto and Heymach[16] described activating *NOTCH1* mutations that defined a distinct subgroup of patients with AdCC who had propensity for bone and liver metastasis and poor prognosis, but also potential responses to Notch1 inhibitors.[17]

Metatypical AdCC has recently been recognized as a morphologic variant of AdCC with a predilection for the sinonasal mucosa. It is characterized by unusual growth patterns including squamous differentiation and macrocystic growth,[18] and striking tubular epithelial hypereosinophilia with luminal cell prominence.[19] This contrasts with the majority of AdCCs, which are basaloid with myoepithelial cell predominance. Metatypical AdCCs have been shown to be characterized by both canonical *MYB/MYBL1:NFIB* and novel *EWSR1:MYB* and *FUS:MYB* gene fusions.[18,19] In our previous study, we have detected an in-frame *EWSR1ex6:MYBex2* and *ACTN4ex18:MYBex2* gene fusions in AdCC with metatypical phenotype in 1 case each.[6]

In the current study, we collected a cohort of 88 cases of sinonasal AdCC. Mutation analysis and detection of fusion transcripts were performed using the TruSight Oncology 500 Kit and/or fluorescence in situ hybridization (FISH) to search for new fusions and mutations, particularly in *NOTCH,* and aiming at identification of potentially targetable genetic alterations associated with AdCC. We also correlated molecular and morphologic findings, with particular reference to identification of high-grade, solid/basaloid, and metatypical phenotypes of sinonasal AdCC.

MATERIALS AND METHODS

Case Selection

A retrospective search in the authors´ registry was conducted, and all sinonasal tumors with features of ad-

TABLE 1. PCR Primers for HPV Detection

HPV	type 16	TCA AAA GCC ACT GTG TCC TGA
		CGT GTT CTT GAT GAT CTG CAA
	type 18	CCG AGC ACG ACA GGA ACG ACT
		TCG TTT TCT TCC TCT GAG TCG CTT
	type 31	CTA CAG TAA GCA TTG TGC TAT GC
		ACG TAA TGG AGA GGT TGC AAT AAC CC
	type 33	AAC GCC ATG AGA GGA CAC AAG
		ACA CAT AAA CGA ACT GTG GTG
	type 35	CCC GAG GCA ACT GAC CTA TA
		GGG GCA CAC TAT TCC AAA TG
	CPSGB	ATATGTCTGAG CCTCCWAARTT
		ATGTTAATWSAGCCWCCAAAATT
		TTA TCA WAT GCC CAY TGT ACC AT
	GP5+	TTTGTTACTGTGGTAGATACTAC
		GAAAAATAAACTGTAAATCATATTC

enoid cystic carcinoma (AdCC) were evaluated histologically and immunohistochemically (A.S. and M.B.). In total, 100 cases were retrieved from the consultation files of the Tumor Registry at the Department of Pathology, Faculty of Medicine in Pilsen and Bioptic Laboratory Ltd in Pilsen, Czech Republic, and tumor registries of the coauthors. Detection of HPV DNA was performed using a set of several PCRs with different primers (Table 1) to cover a wide range of high-risk and low-risk HPV types.

Eleven HPV positive cases were excluded from the study and diagnosed as HPV-associated multiphenotypic carcinoma. One tumor was excluded based on additional clinical information indicating a primary AdCC in the submandibular gland with secondary involvement of the sinonasal area.

Thus, a cohort of 88 cases of sinonasal AdCC was included in this study for further characterization. The tumors were examined histologically, immunohistochemically, and by NGS and/or FISH to detect *MYB*/*MYBL1* and/or *NFIB* gene fusions, as well as any novel gene fusions/mutations. When available, clinical follow-up was obtained from the patients, their physicians, or referring pathologists.

This study was approved by the Ethics Committee of the Faculty Hospital in Pilsen and Charles University, Faculty of Medicine in Pilsen, Czech Republic, on August 2, 2018. Informed consent was not required.

Histologic and Immunohistochemical Studies

For conventional microscopy, excised tissues were fixed in formalin, processed routinely, embedded in paraffin (FFPE), cut, and stained with hematoxylin and eosin.

For immunohistochemistry, 4-μm-thick sections were cut from paraffin blocks and mounted on positively charged slides (TOMO; Matsunami Glass IND, Osaka, Japan). Sections were processed on a BenchMark ULTRA (Ventana Medical Systems, Tucson, AZ), deparaffinized and subjected to heat-induced epitope retrieval by immersion in a CC1 solution (pH: 8.6) at 95°C. All primary antibodies used in this study are summarized in Table 2.

Visualization was performed using the ultraView Universal DAB Detection Kit (Roche, Tucson, AZ) and ultraView Universal Alkaline Phosphatase Red Detection Kit (Roche). The slides were counterstained with Mayer's hematoxylin. Appropriate positive and negative controls were used.

Grading

Three grading systems based on the presence of solid components have been recognized: the Perzin/Szanto system,[20,21] the Spiro system,[22] and the van Weert system.[23] These systems describe the presence of solid components as negative prognosticators at thresholds of 30%, 50%, and any solid component, respectively. All schemes were applied on our cohort, as depicted in Table 3.

Molecular Studies

TruSight Oncology 500 Kit (TS500)

Mutation analysis and fusion-transcript detection were performed using the TruSight Oncology 500 Kit (Illumina, San Diego, CA). RNA was extracted using the Maxwell RSC DNA FFPE Kit and the Maxwell RSC Instrument (Promega, Madison, WI) according to the manufacturer's instructions and quantified using the Qubit HS RNA Assay Kit (Thermo Fisher Scientific, Waltham, MA). DNA was extracted using the QIAsymphony DSP DNA Mini Kit (Qiagen, Hilden, Germany) and quantified using the Qubit BR DNA Assay Kit (Thermo Fisher Scientific). The quality of DNA was assessed using the FFPE QC kit (Illumina), and the quality of RNA was assessed using Agilent RNA ScreenTape Assay (Agilent,

TABLE 2. Antibodies Used for Immunohistochemical Study

Antibody specificity	Clone	Dilution	Antigen retrieval/time	Source
AE1/3	AE1/AE3+PCK26	RTU	EnVision High pH /30 min	Dako
CK7	OV-TL 12/30	1:800	EnVision High pH/30 min	Dako
CK14	SP53	1:800	EnVision High pH/30 min	Cell Marque
p63	DAK-p63	RTU	EnVision Low pH/30 min	Dako
p40	DAK-p40	RTU	EnVision Low pH/30 min	Dako
SOX10	SP267	RTU	CC1/64 min	Cell Marque
Ki-67	MIB-1	RTU	EnVision Low pH/30 min	Dako
MYB	EP769Y	1:100	CC1/64 min	AbCam
S100	Polyclonal	RTU	EnVision Low pH/30 min	Dako
P16	R15-A	1:100	EnVision Low pH/30 min	DB Biotech

CC1 indicates EDTA buffer pH 8.6 at 95°C; EnVision High pH 9.0 at 97°C; EnVision Low pH 6.0 at 97°C; RTU, ready to use.

TABLE 3. Grading Systems Recognized for Adenoid Cystic Carcinoma

Perzin/Szanto* Grade	Our cohort No. of cases (%)	Spiro et al Grade	Our cohort No. of cases (%)	Van Weert et al Grade	Our cohort No. of cases (%)
I. Predominantly tubular, no solid	5 (6)	I. Mostly tubular or cribriform, occasional solid	55 (63)	Low grade—no solid component	22 (25)
II. Predominantly cribriform, < 30% solid	34 (39)	II. Mixed with substantial solid (> 50%)	22 (25)	High grade—any solid component	66 (75)
III. Solid component > 30%	49 (56)	III. Only Solid	11 (13)		

Santa Clara, CA). DNA samples with Cq < 5 and RNA samples with DV200 ≥ 20 were used for further analysis. After enzymatic fragmentation of DNA with KAPAFrag Kit (KAPA Biosystems, Wilmington, MA), DNA and RNA libraries were prepared using the TruSight Oncology 500 Kit (Illumina) according to the manufacturer's protocol. Sequencing was performed on the NovaSeq. 6000 sequencer (Illumina) following manufacturer´s recommendations. Data analysis was conducted using the TruSight Oncology 500 v2.2 Local App (Illumina). Variant annotation and filtering were performed using the Omnomics NGS analysis software (Euformatics, Espoo, Finland). A custom variant filter was set up, including only nonsynonymous variants with coding sequences and a read depth > 50, while benign variants according to the ClinVar database[24] were excluded. The remaining subset of variants was checked visually, and suspected artefactual variants were excluded.[25]

TABLE 4. Clinicopathologic Characteristics of All Patients Qith Sinonasal AdCC (No = 88)

		RNA panel				FISH		DNA panel		
Gene alterations	**Total (%)**	***MYB: NFIB***	***MYBL1: NFIB***	**Noncanonical fusions**	**Fusion/ break negative**	***MYB, NFIB, EWSR1* break***	**NA/ND**	**Mutations oncogenic**	**Gene mutations of UPS**	**NA/ND**
Number of cases (%)	**88** (100)	49 (57)	9 (10)	4 (4)	6 (7)	9 (10)	11 (13)	21/31 (68)	24/31 (77)	57
Age (y)										
< 60	38	23	4	1	2	4	4	11	11	24
More than 60	48	24	5	3	4	5	7	10	13	31
Unknown	2	2	0	0	0	0	0	0	0	2
Median	58.8									
Range	20-86									
Sex										
Male	45	26	4	4	2	3	6	11	12	29
Female	41	21	5	0	4	6	5	10	12	26
Unknown	2	2	0	0	0	0	0	0	0	2
Primary tumor site										
Nasal cavity	49	28	7	2	4	5	3	13	13	31
Maxillary sinus	26	14	1	1	1	3	6	4	7	17
Sphenoid sinus	8	5	1	1	0	1	0	3	3	5
Ethmoid sinus	4	2	0	0	1	0	1	1	1	3
Nasopharynx	1	0	0	0	0	0	1	0	0	1
Follow-up available (mo)	**60**									
Range	1-276									
Mean	62.7									
Outcome	**60**									
Alive NED	18	11	2	1	3	0	0	7	7	7
Alive WD	9	8	1	0	0	0	1	5	4	4
DOD	18	10	1	2	0	2	3	4	4	12
DOC	4	2	0	0	0	2	0	0	0	4
Lost to FU	11	6	1	0	1	2	1	2	3	8
Not available	28	12	4	1	2	3	6	5	6	22
Metastases	14	9	2	0	0	2	1	4	3	9
Recurrences	26	16	1	2	3	2	2	12	10	12

*Fusion negative cases, but harboring *MYB* (No = 7), *NFIB* (No = 1), *or EWSR1* (No = 1) gene break.

AdCC indicates adenoid cystic carcinoma; DOC, dead of other causes; DOD, Dead of disease; FU, follow-up; NA, not analyzable; ND, not done because tissue was not available; NED, no evidence of disease; UPS, uncertain pathogenetic significance; WD, alive with disease.

TABLE 5. The Clinical, Pathologic, and Molecular Genetic Features of 23 Cases of AdCC Harboring Noncanonical Gene Fusions and Oncogenic/Likely Pathogenic Mutations

Case	Age/ sex	Site	FISH	Oncogenic alterations detected by DNA sequencing	Oncogenic alterations detected by RNA sequencing	Therapy	Follow-up period (mo)	Clinical outcome (mo)
1	60/F	Left maxillary sinus		*BCOR* c.4017_4018insT p. (Asp1340Ter) AF: 8%; *RUNX1* c.474_477dup p.(Asp160Ter) AF: 33%	*MYB:NFIB*; exon 13:9; in-frame; NM_001130173; NM_001190737; chr6:135521553; chr9:14116345, Hg19	Medial maxillectomy; protone therapy;	53 AWD	Recurrence (15)
2	72/M	Nasal cavity		*PDGFRA* c.2021C > T p.(Thr674Ile), AF:8% (SAR6)/NA TS500D	*MYB:NFIB,* exon16:exon9, in-frame, NM_001130173.2 NM_00128787.1, *chr6:135539114, chr9:14088325*, Hg19	Endonasal resection; RT	19 NED	NED
3	23/M	Nasal cavity		*GEN1* c.1933_1936del p. (Lys645CysfsTer29) AF: 45% - susp. germline	*MYB:NFIB*; exon 8:10; in-frame; NM_001130173; NM_001190737; chr6:135515598; chr9:14102509, Hg19	Endonasal resection; RT	276 AWD	Recurrence endonasal resection + RT (219) Metastasis left lung with segmentectomy (207)
4	68/M	Maxillary sinus		*BCOR* c.4174-7_4175del AF: 9%; *BCOR* c.1056dup p. (Thr353HisfsTer28) AF: 17%; *BCOR* c.1888_1895del p. (Glu630ProfsTer12) AF: 9%; *RUNX1* c.985del p. (Ala329ArgfsTer265) AF: 19%; *RIT1* c.319A > G p.(Met107Val) AF: 19%	*MYB:NFIB*, exon 8:exon 9, in-frame, NM_001130173.2, NM_001190737.2, chr6:135515598, chr9:14116345, Hg19	NA	NA	NA
5	50/F	Nasal cavity	*MYB* break	*KDM6A* c.2172_2173del p. (Leu725AspfsTer4) AF: 22%; *KDM6A* c.618-619+2del AF: 34%	neg	NA	NA	NA
6	43/M	Left maxillary sinus		*AVCR1B* c.1133dup, p. (Ser379ValfsTer24), AF: 34%	*MYB:NFIB,* exon15:exon10, in-frame, NM_001130173.2, NM_00128787.1, chr6:135524462, chr9:14102509, Hg19	Radical surgery, CHT	60 AWD	
7	71/M	Nasal cavity		*KDM6A* c.64del, p. (Glu22LysfsTer20), AF: 13%; *SMARCA4* c.3580G > T, p. (Gly1194Trp), AF: 13%	*MYB:NFIB,* exon8:exon10, in-frame, NM_001130173.2, NM_00128787.1, chr6:135515598, chr9:14102509, Hg19	Nonradical excision, RT	5 DOD	Meta (5)
8	35/M	Nasal cavity, sinuses		BCOR c.3669_3673del, p. (Ala1224ArgfsTer19), AF: 52% - susp. germline;	MYB:NFIB, exon13:exon11, in-frame, NM_001130173.2, NM_00128787.1, chr6:135521553 , chr9:14088325, Hg19	Radical surgery, RT	60 AWD	Recurrence (50) Meta right lung (60)
9	60/F	Maxillary sinus		*ARID1A* c.1680_1682del p. (Tyr560_Gln561delinsTer), AF: 34%; *EP300* c.3355del p. (Asp1119MetfsTer38), AF: 66%; *NOTCH1* c.7399_7405del p. (Ser2467HisfsTer8), AF: 34%, *NOTCH1* c.5722_5725del p. (Ala1908SerfsTer72), AF: 33%	*MYB:NFIB,* exon13:exon10, in-frame, NM_001130173.2, NM_00128787.1, chr6:135521553 , chr9:14102509, Hg19	Radical surgery, RT	20 DOD	Recurrence (3x) Tumor in infratemporal fossa, resected (10); tumor in maxillary bone, soft tissues (12); Tumor in supraorbital and ethmoidal area (20)
10	55/M	Maxillary sinus		no *P*/LP variant	*ESRRG:DNM3,* exon3: exon14 , frame unknown, NM_001134285.1, NM_015569.5, chr1:217112924, chr1:172100315, Hg19 at the limit of detection	Radical surgery, RT	72 DOD	Recurrence (24)
11	55/F	Sphenoid sinus	*NFIB* break	*PPM1D* c.1218del p. (Cys407ValfsTer2), AF: 14%; *SMARCA4* c.2644G > A p. (Glu882Lys), AF: 13%; *LZTR1* c.1210G > A p.(Gly404Arg), AF: 11%	neg	Radical surgery, RT	24 LOF	
12	55/M	Nasal cavity		*MGA* c.6815del p. (Gly2272ValfsTer63), AF: 41%; *EP300* c.1811G > A p. (Arg604Gln), AF: 10%	*MYB:NFIB*, exon 15:exon 11, in-frame, NM_001130173.2, NM_00128787.1, chr6:135524462, chr9:14102509, Hg19	Surgery, RT	144 DOD	Recurrence (12); meta liver (120); local progression (140)
13	62/M	Nasal cavity		no *P*/LP variant	*ACTB:MYB,* exon 3:3; in-frame; NM_001101; NM_001130173; chr7:5568792; chr6:135508972, Hg19	Surgery, proton therapy	103 NED	
14	46/F	Nasal	neg	*RB1* c.1939_1940del p.	neg	Surgery, RT,	98 AWD	Recurrence

TABLE 5. (*continued*)

Case	Age/ sex	Site	FISH	Oncogenic alterations detected by DNA sequencing	Oncogenic alterations detected by RNA sequencing	Therapy	Follow-up period (mo)	Clinical outcome (mo)
		cavity		(Leu647PhefsTer5), AF: 18%		CHT		
15	68/F	Nasal cavity		PHF6 c.1039C > T, p.(Arg347Ter), AF: 49% - susp. germline	*MYB:NFIB*, exon 8:exon 11, in-frame, NM_001130173.2, NM_001190737.2, chr6:135515598, chr9:14088325, Hg19	Radical surgery, RT	NA	NA
16	82/M	Sphenoid sinus		*PTEN* c.32_33del, p. (Arg11LysfsTer32), AF: 31%,	*EWSR1:MYB,* exon 6:exon 2, in-frame, NM_005243.4, NM_001130173.2, chr22:29678546, chr6:135507041, Hg19	Surgery, RT	84 DOD	Recurrence
17	57/M	Nasal cavity		*SPEN* c.2918dup p. (Ser974LysfsTer48), AF: 26%; *CREBBP* c.2489del p. (Pro830LeufsTer19), AF: 22%; EP300 c.1927G > T p.(Glu643Ter), AF: 24%; *DDX41* c.121C > T p. (Gln41Ter), AF: 45% - susp. germline; *NOTCH1* c.7177C > T p. (Gln2393Ter), AF: 22%	*MYB:NFIB*, exon 15:exon 11, in-frame, NM_001130173.2, NM_001190737.2, chr6:135524462, chr9:14088325, Hg19	Surgery, proton therapy	73 AWD	
18	69/M	Nasal cavity		*CHD2* c.4156del p. (Ser1386ValfsTer3) AF: 26%; *ROS1* c.350del p. (Leu117TyrfsTer11) AF: 48% - susp. germline; *TAF1* c.4882-1G > A AF: 6%	*ACTN4:MYB,* exon 18:exon 2, in-frame, NM_004924.6, NM_001130173.2, chr19:39217743, chr6:135510929, Hg19	Surgery, RT	NA	NA
19	76/M	Nasal cavity		*CCND1* c.855C > A, p.(Cys285Ter), AF: 45% - susp. germline	*MYB:NFIB*, exon 15:exon 11, in-frame, NM_001130173.2, NM_00128787.1, chr6:135524462, chr9:14102509, Hg19	Surgery;	72 AWD	Recurrence (48) surgery+RT
20	29/F	Sphenoid sinus		*SPEN* c.2906del p. (Pro969LeufsTer5), AF: 10%	*MYB:NFIB*, exon 13:exon 11, in-frame, NM_001130173.2, NM_001190737.2, chr6:135521553, chr9:14088325, Hg19	Surgery, CHT	NA	NA
21	57/F	Sinonasal NOS		*NOTCH1* c.7400C > A, p. (Ser2467Ter), AF: 24%;	*MYB:NFIB*, exon 8:exon 11, in-frame, NM_001130173.2, NM_00128787.1, chr6:135515598, chr9:14102509, Hg19	Surgery, RT	64 DOD	Recurrence (38)
22	53/F	Ethmoidal sinus	neg	*BCOR* c.3892_3898del, p. (Ser1298ValfsTer69), AF: 49% - susp. germline; NF1 c.1477_1490del, p. (Leu493GlufsTer13), AF: 31%	neg	Surgery, RT	16 LOF	
23	57/F	Nasal cavity		*PALB2* c.172_175del p. (Gln60ArgfsTer7), AF: 44% - susp. germline	*MYBL1:NFIB*, exon 8:exon 10, in-frame, NM_001080416.4, NM_001190737.2, chr8:67504675, chr9:14102509, Hg19	Subtotal left hemimaxilectomy with resection of the nasal base and inferior nasal shell	35 NED	

AWD indicates alive with disease; CHT, chemotherapy; DOD, dead of disease; DWD, dead with disease; F, female; LOF, lost of follow-up; M, male; meta, metastasis; mo, month; NA, not available; NED, no evidence of disease; RT, radiotherapy.

Fluorescence In Situ Hybridization (FISH) Analysis

Before FISH, hematoxylin and eosin-stained slides were examined to determine the areas for cell evaluation. Then, a 4-μm-thick FFPE section was placed onto a positively charged slide. The unstained slide was routinely deparaffinized and incubated in 1× Target Retrieval Solution Citrate pH 6 (Dako, Glostrup, Denmark) for 40 minutes at 95°C, subsequently cooled for 20 minutes at room temperature in the same solution and washed in deionized water for 5 minutes. The slide was digested in protease solution with pepsin (0.5 mg/mL) (Sigma Aldrich, St Louis, MO) in 0.01 mol/L HCl at 37°C for 45 to 60 minutes, depending on sample conditions. The slide was then rinsed in deionized water for 5 minutes, dehydrated in a series of ethanol solutions (70%, 85%, and 96% for 2 min each), and air-dried.

The details of *EWSR1*, *MYB*, *NFIB* break-apart, and *MYB*:*NFIB* fusion analysis have been described previously.[5,26] For the detection of *EWSR1*:*MYB* fusion, custom designed EWSR1:MYB dual fusion probes comprising the catalogue 22q12.2. EWSR1 DF 498 kb probe and custom MYB probe with chromosomal location: chr6:135,271,382-135,771,382 (Agilent Technologies) were used following similar protocols.

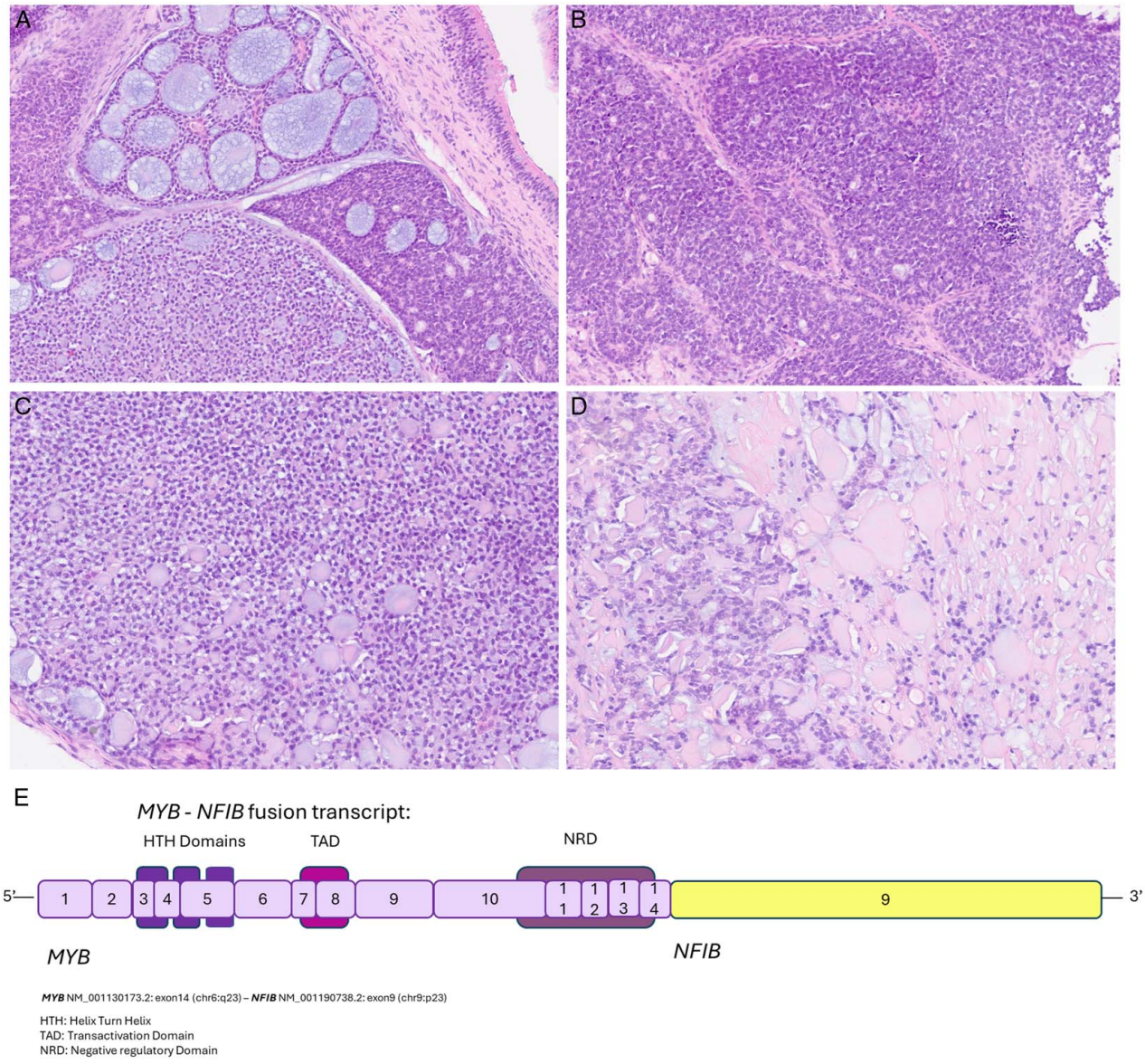

FIGURE 1. AdCC with canonical *MYB:NFIB* gene fusion showed biphasic tumor growth of predominantly cribriform pattern (A) than tubular or more solid areas (B). Both pseudocysts and true glandular lumina were characteristic for AdCC (C). Abundant deposits of a hyalinized eosinophilic extracellular matrix and reduplicated basement membrane materials were often seen (D). The fusion joining of *MYB* gene exon 14 with *NFIB* gene exon 9 is illustrated. Protein domains are depicted (E).

Detection of HPV

For HPV studies, genomic DNA was isolated from formalin-fixed, paraffin-embedded tissue using QIAsymphony SP and special precautions were taken to prevent HPV DNA microcontamination. Briefly, five 5-µm-thick sections were cut from the blocks. A new microtome blade was used each time a new case was sectioned. DNA was extracted by the QIAsymphony DNA Mini Kit (Qiagen) according to manufacturer's protocol. The quality of isolated DNA was checked by PCR which amplifies a set of control genes.[27]

Detection of HPV DNA was performed using a set of several PCRs with different primers (Table 1) to cover a wide range of high-risk and low-risk HPV types. For all samples, the primers' systems targeting both L1 and E1 region were used: CPSGB, GP5+/GP6+, as previously described.[28] To avoid false negative findings (because of loss of L1 or E1 regions due to HPV integration into host genome) PCR targeting HPV oncogenes E6, and E7 of the 6 most prevalent HR-HPV types including types 16, 18, 31, 33, 35, and 45 was performed.[29]

All PCRs were run on the cycler GeneAmp PCR System 9700 (PE/Applied Biosystem, Forster City, CA). Amplicons were analyzed in 2% agarose gel with ethidium bromide. Positive PCR samples were genotyped by hybridizing them to type-specific probes, or sequenced and

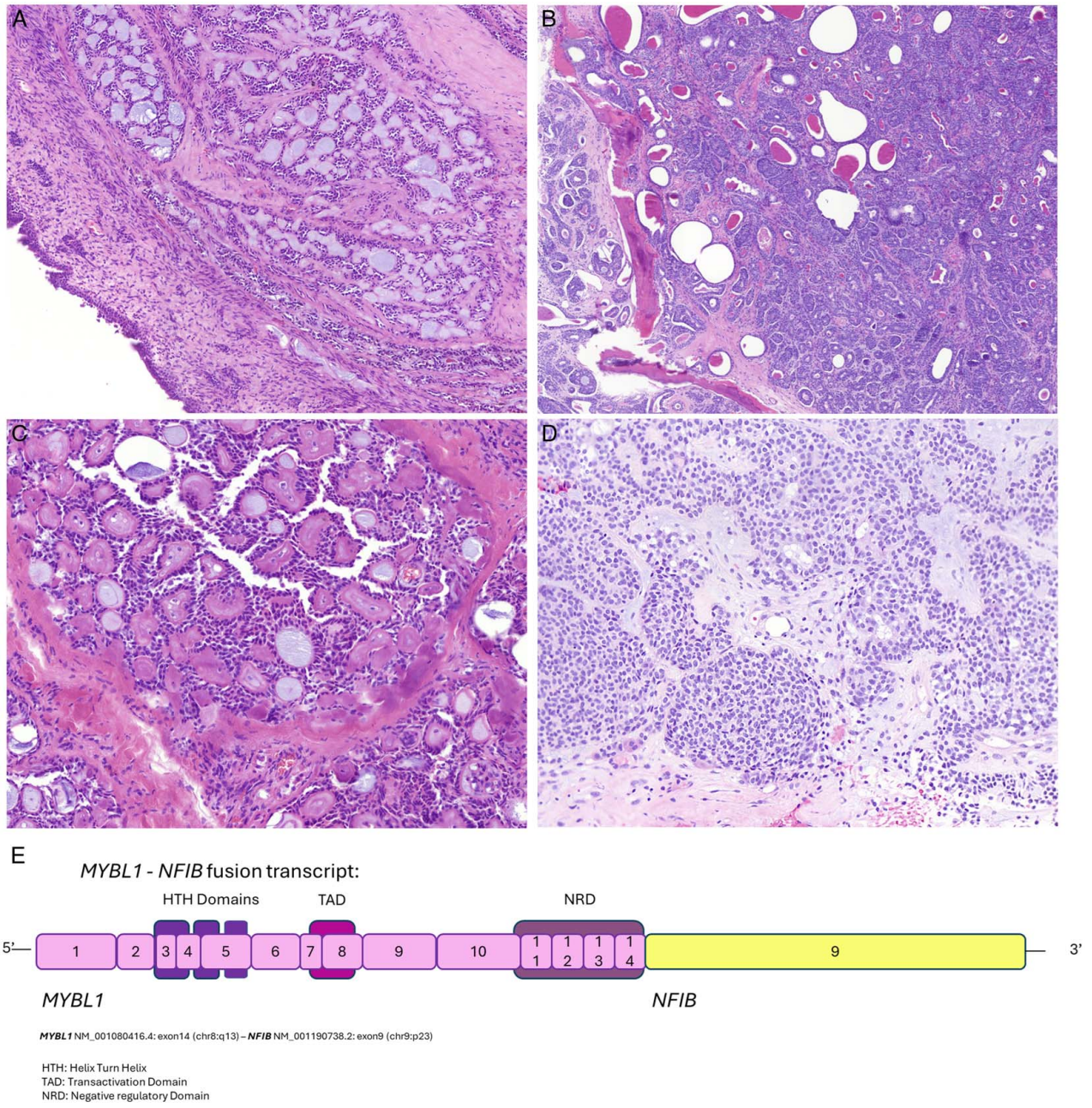

FIGURE 2. AdCC with canonical *MYBL1:NFIB* gene fusion was composed predominantly of combination of cribriform (A) and tubular (B) patters with microcystic-like spaces filled with hyaline or basophilic basement membrane material (C). The solid areas were also present lacking pseudocystic spaces present in previous 2 patters (D). The fusion joining of *MYBL1* gene exon 14 with *NFIB* gene exon 9 is illustrated. Protein domains are depicted (E).

compared with BLAST databases. Positive and negative controls were included in every run.

RESULTS

Demographic and Clinicopathologic Findings

We collected a cohort of 88 cases of sinonasal AdCC. Clinical data, follow-up, and molecular genetic results are summarized in Tables 4 and 5.

The patients comprised 45 men and 41 women (with gender unknown in 2 cases), ranging in age from 20 to 86 years (mean: 58.8 y). The tumors arose in the nasal cavity (49 cases), the maxillary sinus (26 cases), the sphenoid sinus (8 cases), the ethmoid sinus (4 cases), and the nasopharynx (1 case).

Treatment consisted of excision or radical surgical resection in 30/47 (64%) cases. Chemotherapy, radiation and/or proton therapy were administered before surgery,

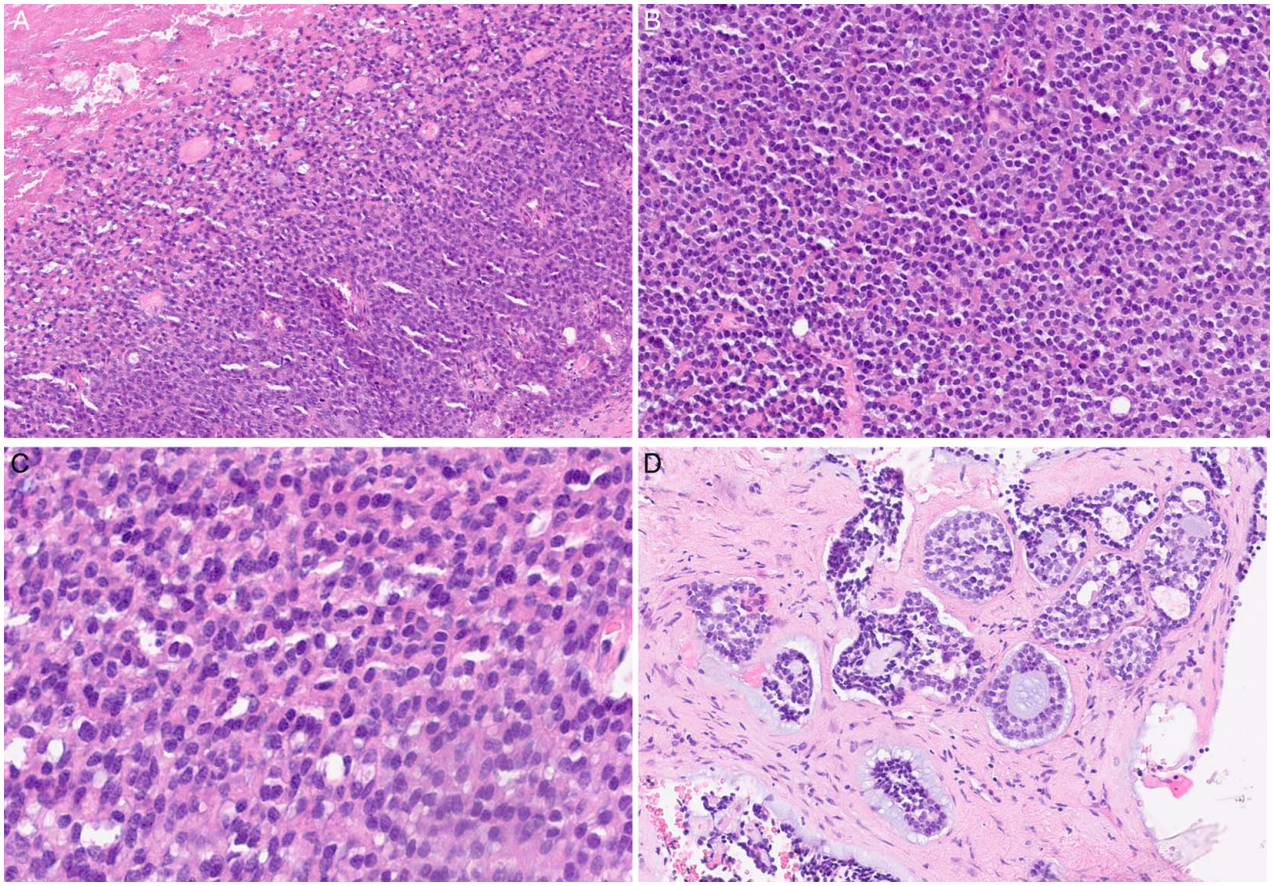

FIGURE 3. The case of *ACTBex3:MYBex3* AdCC the tumor resemble myoepithelial derived neoplasm with hypercellular periphery and necrotic center (A). The tumor cells were basaloid with monomorphic hyperchromatic nuclei (B) and areas with high-grade features consisting of moderately pleomorphic nuclei (C). Conventional cribriform or tubular patterns were present at the periphery of the tumor surrounded by fibrohyaline stroma (D).

after surgery, or as the sole therapeutic approach in 44/49 patients (90%). One patient received targeted therapy with Imatinib. Distant metastatic spread was reported in 14/60 (23%) cases, with one or more metastases in the lung (9 cases), the liver (2 cases), the brain (1 case), bones (pelvis and sacrum, 1 case), or the axilla (1 case). Local recurrence was observed in 26/60 cases (43%) (Table 4).

Follow-up information was available for 60/88 (68%) patients, with follow-up periods ranging from shortly after diagnosis to 276 months (mean follow-up: 62.7 mo). Eighteen patients (18/60, 30%) were alive without evidence of disease (mean follow-up of 91.9 mo), 9 patients (15%) were alive with disease (mean follow-up of 35.6 mo), 18 patients (30%) died of the disease (mean follow-up of 63 mo), 4 patients (7%) died of unrelated causes (mean follow-up of 46.3 mo), and 11 patients (18%) were lost to follow-up after a follow-up period with regular check-ups (mean follow-up of 33.6 mo) (Table 4).

Grading

All 3 grading systems were applied on our cohort. The presence of solid component is independent on the presence of canonical or alternative gene fusion. In our cohort, 49 cases showed more than 30% solid component, 33 cases showed more than 50%, and 66 cases showed any amount of solid component. The presence of a solid component was independent of the presence of canonical or alternative gene fusions. The total amount and categorization of our cohort into 3 independent grading systems is depicted in Table 3. High-grade transformation/dedifferentiation was not present.

Molecular Findings

Sinonasal AdCC was predominantly characterized by canonical *MYB:NFIB* (49 cases) (Fig. 1E) and *MYBL1:NFIB* (9 cases) (Fig. 2E) fusions. In addition, rearrangements in *MYB* (8 cases), *NFIB* (1 case), and *EWSR1* (1 case) genes were detected in 9 cases using FISH. NGS analysis revealed novel noncanonical fusion transcripts, including *ACTB:MYB; ACTN4:MYB; ESRRG:DNM3,* and *EWSR1:MYB*, each in 1 case.

Mutational analysis was performed by NGS in 31/88 (35%) AdCCs. Mutations in genes with established roles in oncogenesis were identified in 21/31 tumors (68%), including *BCOR* (4/21; 19%), *NOTCH1* (3/21; 14%), *EP300* (3/21; 14%), *SMARCA4* (2/21; 9%), *RUNX1* (2/21; 9%),

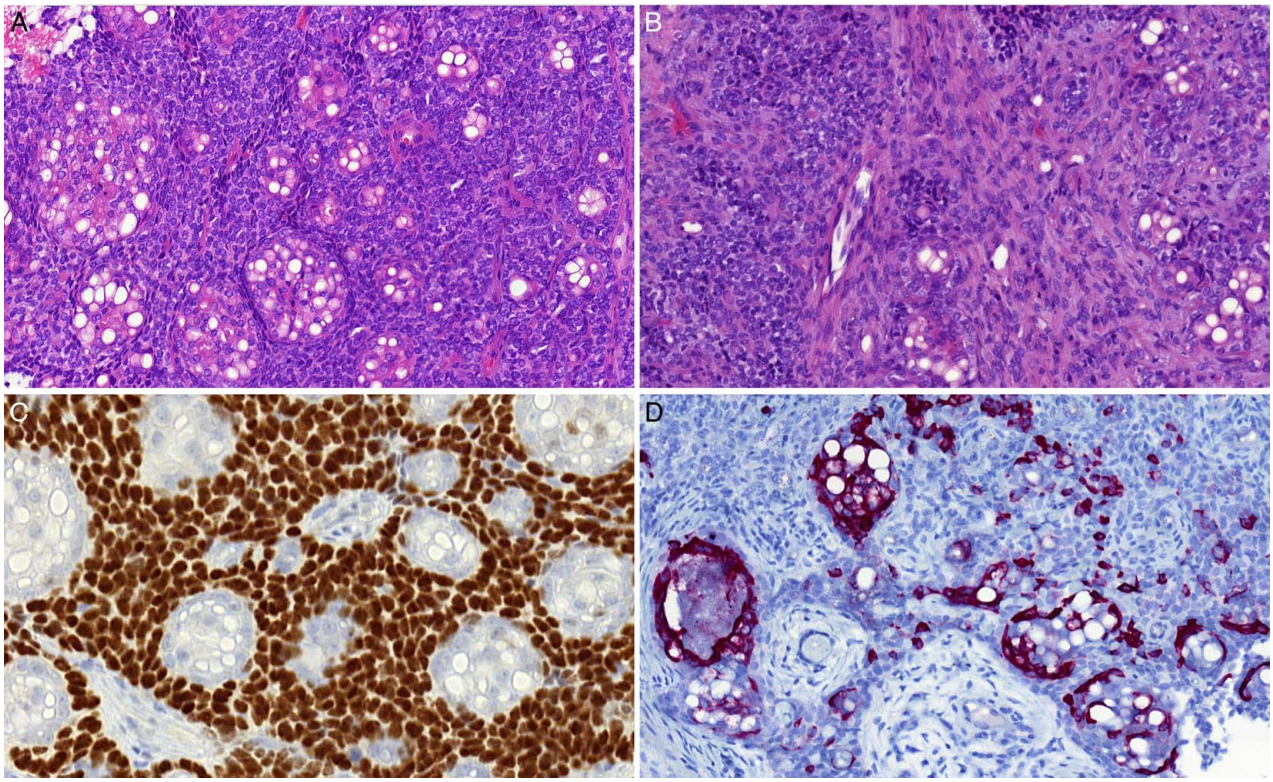

FIGURE 4. A, The AdCC with in-frame *ACTN4ex18:MYBex2* gene fusion consisted of 2 types of tumor cells with predominant monomorphic and basaloid cells and groups of vacuolated cells. B, Stromal component was minor and characterized by mild cellular fibrous bands with distended vascular spaces dispersed throughout the tumor. C, Basaloid tumor cells were positive for p63. D, Vacuolated (clear) cells showed CK7 expression.

KDM6A (2/21; 9%), *SPEN* (2/21; 9%), and *RIT1, MGA, RB1, PHF6, PTEN, CREBBP, DDX41, CHD2, ROS1, TAF1, CCD1, NF1, PALB2, AVCR1B, ARID1A, PPM1D, LZTR1, GEN1*, *PDGFRA*, each in 1 case (1/21; 5%). In addition, 24/31 (77%) cases exhibited a spectrum of gene mutations of uncertain pathogenetic significance. Moreover, no known pathogenic mutations were detected in 9/31 (29%) cases. None of the detected mutations occurred at a high level of recurrence. Even the most frequent mutations of *BCOR* and *NOTCH1* showed a low level of recurrence at 19% and 14%, respectively, in our AdCC cases as a whole.

The clinical features of all 23 cases of AdCC harboring noncanonical gene fusions and oncogenic/likely pathogenic mutations are summarized in Table 5. The clinical outcome of patients with *NOTCH* and *BCOR* mutated AdCCs was notably poor. There were 3 patients with *NOTCH*-mutated AdCCs, and 2 of them experienced multiple recurrences, and died of disease at 20 and 64 months, respectively. One patient is currently alive and receives proton therapy, with brain metastasis at 5 months after primary diagnosis. Two of 4 patients with *BCOR* mutated AdCC are alive with disease at 53 and 60 months respectively, but both have experienced local recurrences at 53 and 50 months, and 1 is alive with lung metastasis, while 2 patients were lost to follow-up (Table 5).

Histopathologic and Immunohistochemical Findings

Sinonasal Adenoid Cystic Carcinomas With Canonical *MYB*/*MYB1:NFIB* Gene Fusions

Histologically, there was no morphologic difference between AdCCs with *MYBL1:NFIB* and those with *MYB:NFIB* fusion. All these fusion-positive sinonasal AdCCs exhibited an infiltrative biphasic growth pattern consisting of both ductal epithelial and myoepithelial cells. Identification of both pseudocysts and true glandular lumina was required to make the diagnosis. The most common architectural patterns, namely cribriform, tubular, and solid were observed in varying proportions. The cribriform pattern was the most prevalent in both molecular subtypes *MYB:NFIB* and *MYBL1:NFIB,* as illustrated in Figures 1A and 2A,C, respectively. The cribriform/pseudocystic growth pattern is characterized by nests of tumor cells with microcystic-like spaces filled with hyaline basement membrane-like or basophilic mucoid material. The solid pattern, characterized by tumor sheets composed of basaloid cells lacking tubular or cribriform formations, was also observed in both subtypes of AdCC with canonical fusion transcripts (Fig. 1B, Fig. 2D). Combinations of these growth patterns were common (Fig. 1C). Abundant deposits of hyalinized eosinophilic

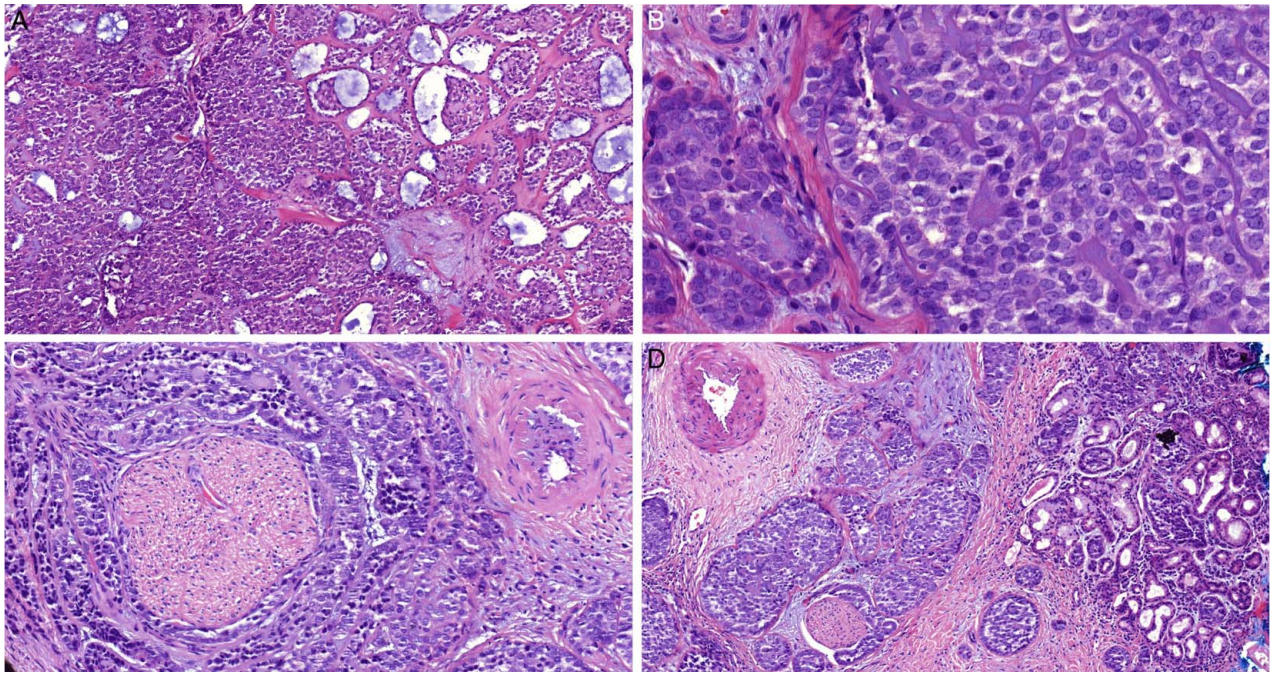

FIGURE 5. A, The case of *ESRRGex3:DNM3ex14* translocated AdCC consisted of different architectural patterns including solid, tubular, micropapillary, and cribriform. B, Tumor cells were pleomorphic with visible nucleoli, nuclear hyperchromasia, and focally vacuolated cytoplasm. C, Aggressive appearance of the tumor was supported bymassive targetoid perineural spread. D, A transition zone contained atypical sinonasal glands arising from the respiratory adenomatoid hamartoma.

extracellular matrix and reduplicated basement membrane materials were often seen (Fig. 1D). The tubular pattern, consisting of well-formed ducts and tubules lined by luminal ductal and abluminal myoepithelial cells, was the least common growth pattern (Fig. 2B).

Sinonasal Adenoid Cystic Carcinomas With Noncanonical Fusion

We identified 4 cases of sinonasal AdCC harboring novel noncanonical fusion transcripts, namely *ACTB:MYB, ACTN4:MYB*, *ESRRG:DNM3,* and *EWSR1:MYB.*

Two cases with fusions involving *ACTB* and *ACTN4* genes predominantly exhibited a solid growth pattern of monomorphic basaloid cells without significant nuclear atypia. In the former of those 2 (in-frame *ACTBex3:MYBex3* fusion), the tumor fragments were 8 cm in the largest diameter and displayed a macroscopic mucinous appearance. Microscopic examination revealed a polypoid and partly cystic lesion of predominantly myoepithelial appearance with lobulated multinodular architecture, a hypercellular periphery and hypocellular center with large necrotic areas (Fig. 3A). Tumor cells were basaloid and had monomorphic hyperchromatic nuclei (Fig. 3B) with high-grade features (Fig. 3C). Areas of conventional cribriform adenoid cystic carcinoma were present at the periphery and represented 20% of the tumor mass (Fig. 3D). The stroma was partly hyalinized and partly myxoid. The growth pattern was biphasic with p63 positivity in the cells of the abluminal component. Ki-67 proliferation index was estimated at 30%.

The latter case represented an example of metatypical AdCC (in-frame *ACTN4ex18:MYBex2* fusion, and a break of the *MYB* gene). The tumor consisted of a solid tumor mass composed of 2 cell populations. The predominant component was composed of monomorphic basaloid cells without significant nuclear atypia or mitotic activity. A less frequent cell population was represented by groups of cells with pale eosinophilic to vacuolated cytoplasm (Fig. 4A). These cells were identical both in morphology and immunoprofile with cells described by Altemani et al.[30] A stromal component was minor and characterized by fibrous bands with distended vascular spaces and large areas of dense sclerosis with mucoid material (Fig. 4B). Basaloid tumor cells were positive for p63 (Fig. 4C) and CK14. Vacuolated (clear) cells showed CK7 expression (Fig. 4D). Ki-67 proliferation index was estimated at 2%.

The third case featuring a novel *ESRRGex3:DNM3ex14* fusion not previously described in AdCC was a polypoid lesion infiltrating the right maxilla. The tumor consisted of a main tumor mass corresponding to conventional AdCC while areas in the periphery of the lesion resembled a seromucinous hamartoma.[31] The AdCC component of the lesion comprised different architectural patterns, including solid, tubular, micropapillary, and cribriform (containing hyaline or basophilic mucoid material) (Fig. 5A). Areas of stromal edema or fibromyxohyaline change of the interstitium contained small clusters, cords, or isolated tumor cells, that were sometimes bizarre. The AdCC tumor cells were pleomorphic

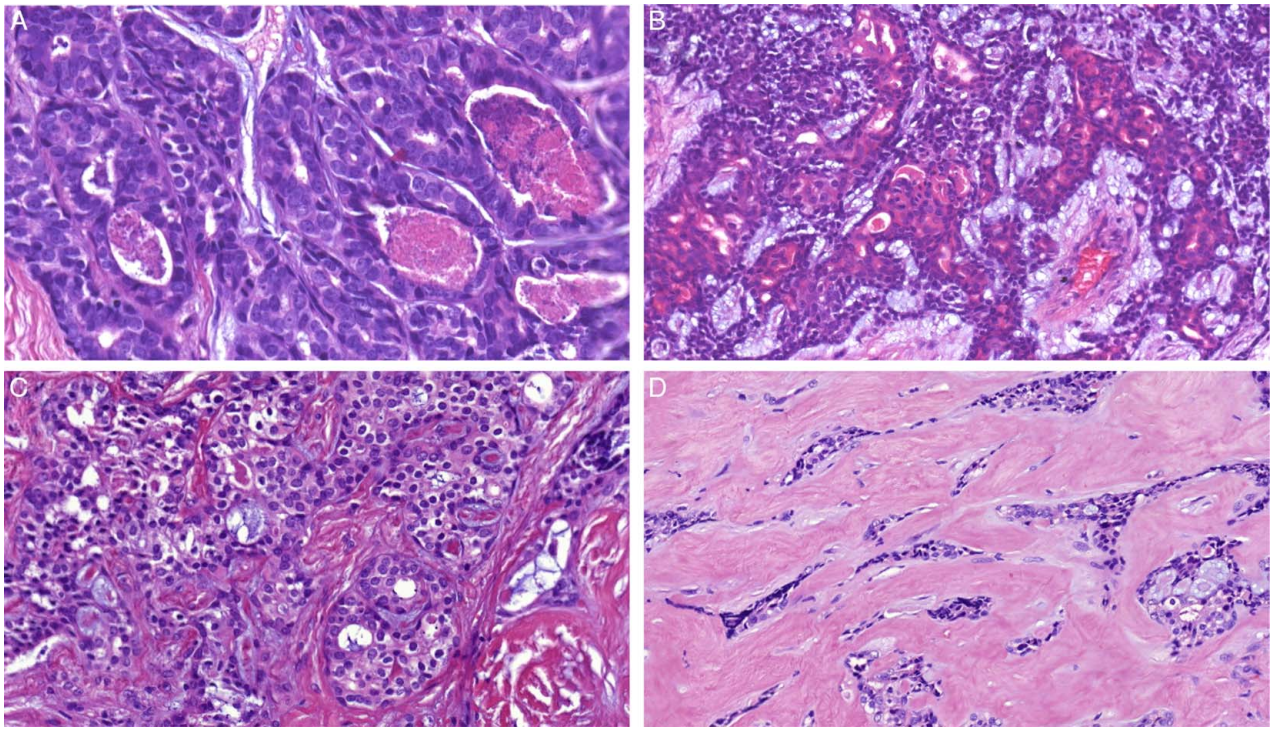

FIGURE 6. The AdCC with in-frame *EWSR1ex6:MYBex2* gene fusion was in part composed of cellular areas of basaloid cells forming tubular and cribriform patterns with multiple areas of comedo-like necrosis (A), focally with extensive tubular hypereosinophilia (B) and foci of intraluminal clear cells (C) separated by fibrous bands. In part, the tumor consisted of hypocellular characterized by fibrosclerotic and hyalinized stroma with focal myxoid change and cords and ducts of tumor cells (D).

with irregular nuclear borders, nuclear hyperchromasia, or chromatin clearing with prominent nucleoli and nuclear grooves. The cytoplasm was eosinophilic to clear and bubbly (Fig. 5B). Perineural invasion was prominent (Fig. 5C). Mitotic activity was high. A transition zone contained atypical sinonasal glands arising from the respiratory adenomatoid hamartoma-like periphery (Fig. 5D) connected to the AdCC tumor mass.

The fourth case was an 82-year-old man with a tumor mass of the sphenoid sinus (in-frame *EWSR1ex6:MYBex2*). This case was reported in a previous cohort of metatypical AdCC.[18] The tumor was composed of hypercellular and hypocellular areas. The hypercellular areas consisted of basaloid cells forming tubular and cribriform patterns with multiple areas of comedo-like necrosis (Fig. 6A), extensive tubular epithelial hypereosinophilia (Fig. 6B), and foci of intraluminal clear cells (Fig. 6C). The islands of tumor cells were circumscribed by basement membrane deposits or basophilic mucoid material. The hypocellular area was composed of fibrosclerotic and hyalinized stroma with focal myxoid change and cords and ducts of tumor cells (Fig. 6D). Tumor cells were pleomorphic with irregular nuclear borders, nuclear grooves, and multiple nucleoli. The cytoplasm was eosinophilic to clear. Tumor cells showed typical biphasic immunohistochemical pattern with the luminal cells positive for CK7, while the abluminal cells were positive for p63, CK14, and SOX10. Proliferative activity was mostly intermediate, but reached up to 25% in hot spot regions.

Sinonasal Adenoid Cystic Carcinomas With *NOTCH* Gene Family Mutations

Three cases of AdCC harbored mutations in *NOTCH1* gene. These tumors were characterized by a predominant solid growth pattern, nuclear enlargement, and polymorphism (Fig. 7A). There were nests forming confluent sheets of tumor cells, and comedonecrosis was pronounced (Fig. 7B). Mitotic and Ki-67 labeling indices were significantly higher in solid areas as compared with cribriform/tubular pattern in conventional AdCC (Figs. 7C–D). Two *NOTCH*-mutated AdCCs exhibited metatypical features, including unusual growth patterns with squamous differentiation (Fig. 8A), tubular epithelial hypereosinophilia with luminal cell prominence (Fig. 8B), and focal sebaceous metaplasia (Fig. 8C). In one metatypical AdCC, multiple foci of foamy vaculated eosinophilic cells were present within the nests composed of basaloid neoplastic cells (Fig. 8D).

Our cohort included 31/88 (35%) cases of AdCC (with canonical or noncanonical fusions) associated with seromucinous hamartoma (SH) and/or atypical sinonasal glands arising in SH (ASGSH) (Fig. 5D).[31] The nuclei varied in size and shape and were often hyperchromatic. Forty-four of 88 (50%) cases consisted of a pure AdCC tumor mass with no evidence of surface or other structures of normal mucosa. In 11 cases, a normal sinonasal epithelium with no atypia covered the tumor mass. In 4 additional cases, squamous epithelium without dysplasia lined the surface of some tumor fragments.

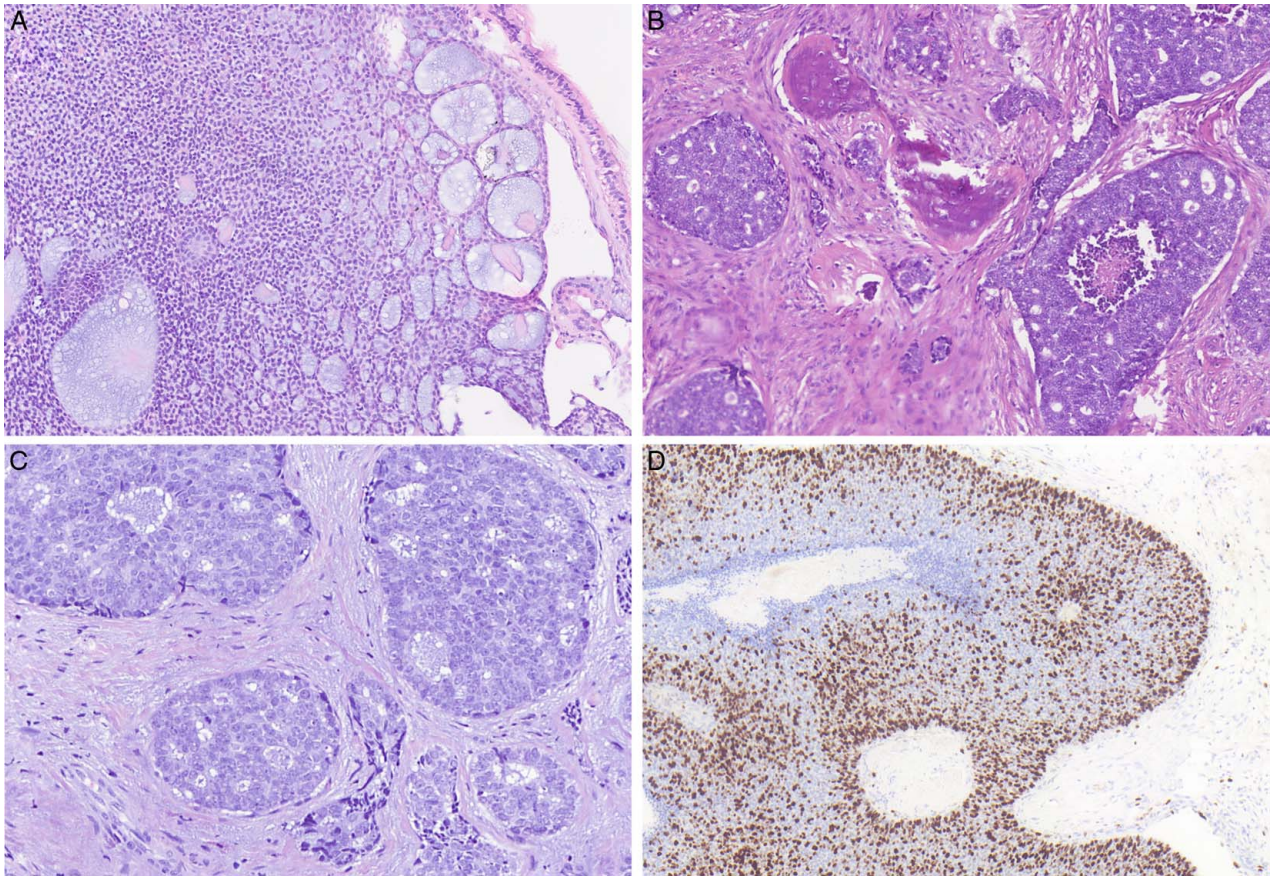

FIGURE 7. A, The cases of AdCC with *NOTCH1/3* mutation were predominantly of solid growth focally with pseudocysts filled with basophilic mucoid material. B, The solid areas showed comedonecrosis and were embedded in desmoplastic stroma with bone invasion. C, Conventional cribriform or tubular patterns were less encountered. D, Ki-67 index was high in solid areas.

DISCUSSION

Adenoid cystic carcinoma (AdCC) is one of the most common salivary gland malignancies, found in both major and minor salivary and seromucous gland sites. Historically, AdCCs of salivary gland origin have been categorized as fusion-defined carcinomas due to the consistent presence of *MYB:NFIB* fusion genes in over 80% of the cases and *MYBL1:NFIB* in ~5%.[2,3] *MYB*/*MYBL1* activation through gene fusion or other mechanisms is therefore considered a critical event in the pathogenesis of AdCC.[2] Further exploration has unveiled additional partner genes linked to *MYB* and *NFIB,* such as *EWSR1:MYB*, *FUS:MYB*,[19] *MYB:PDCD1LG2*, *MYB:EFR3A*, and *NFIB:AIG1,* respectively,[32] expanding our understanding of AdCC pathogenesis. Intriguingly, some AdCCs lack these rearrangements, raising questions about possible additional fusion-transcript mechanisms. This is particularly important in small biopsy samples, where AdCC might be misdiagnosed as another entity.

In the previous study of our group,[6] NGS analysis revealed noncanonical fusion genes including *ACTB:MYB, ACTN4:MYB, ESRRG:DNM3,* each found in 1 tumor case. In the current study, these data are presented in a more comprehensive manner, along with additional details, including morphology and patient outcomes, that were not provided in the prior study. Interestingly, tumors with these alternative fusion genes appear to associate with an unusual variant of morphologic features. Our cases displayed foci of squamous metaplasia, extensive tubular epithelial hypereosinophilia, and clusters of eosinophilic to clear cells with vacuolated or bubbly cytoplasm, leading to the diagnosis of "metatypical AdCC." This term was introduced by Mathew et al.[18] The authors presented 3 cases of AdCC with unusual features, including extensive squamous differentiation, macrocystic, and trabecular growth patterns, while harboring *MYB*/*MYBL1:NFIB* fusion transcripts.[18] Weinreb et al[19] subsequently expanded the spectrum of metatypical morphologies by including AdCC with foci of striking tubular epithelial hypereosinophilia, present in both cases with canonical and novel *EWSR1:MYB* and *FUS:MYB* fusions. In our series, 3 of previously published cases with noncanonical fusions (*ACTN4:MYB, ACTB:MYB,* and *ESRRG:DNM3*) showed morphologies of metatypical AdCCs.[6] The tumors were composed of different architectural patterns including solid, tubular, micropapillary, and cribriform with predominant component made of monomorphic basaloid cells that showed peripheral

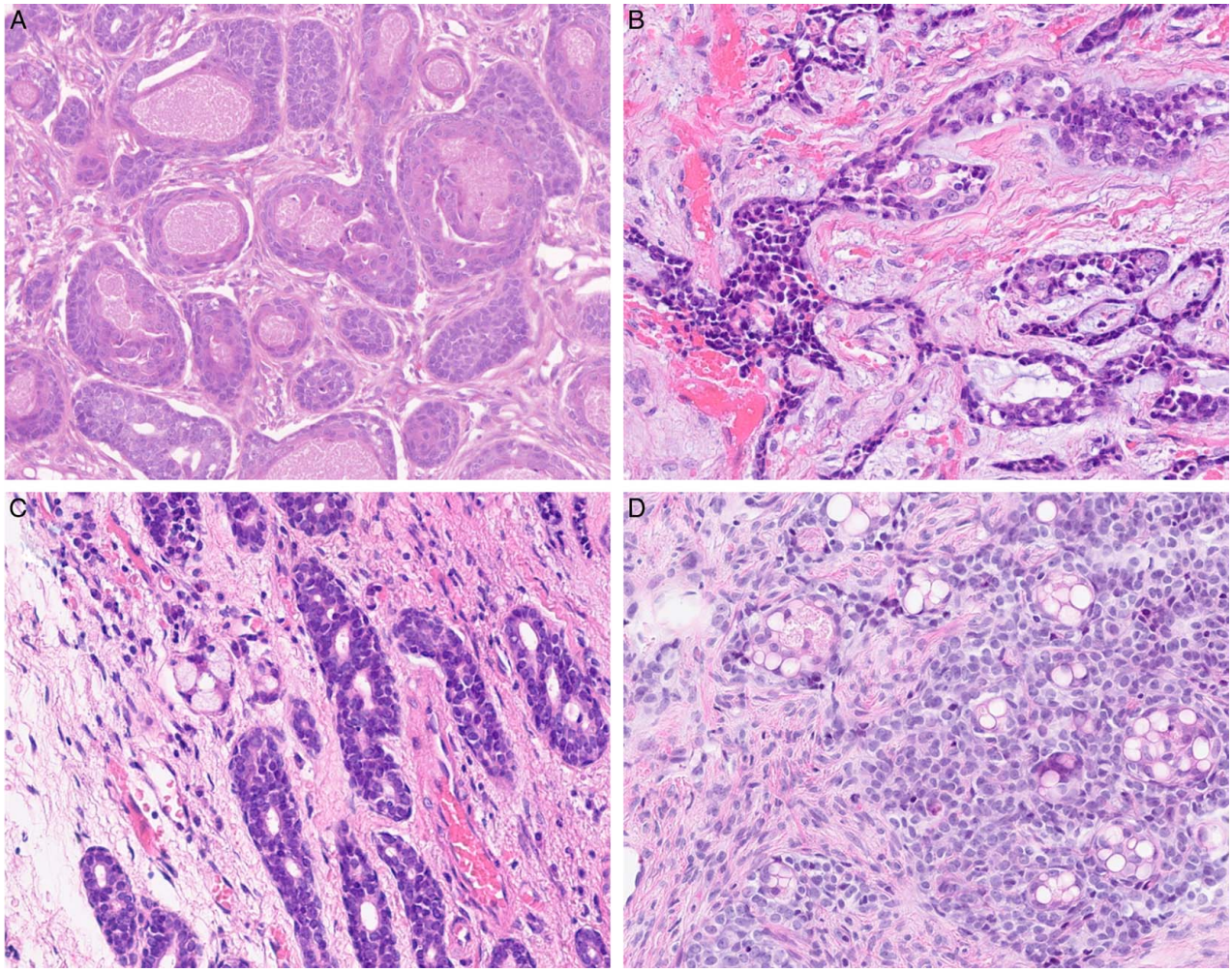

FIGURE 8. The metatypical changes were encountered in 2 AdCC with *NOTCH* mutations showing squamous cell differentiation (A), tubular hypereosinophilia (B), focal sebaceous metaplasia (C), and foamy vacuolated cells (D).

palisading of the nuclei. A less frequent cellular population was represented by groups of cells with pale eosinophilic to vacuolated cytoplasm and extensive tubular hyper-eosinophilia. In addition, we have observed metatypical features, namely sebaceous foci, clusters of eosinophilic and foamy cells, and extensive squamous metaplasia also in AdCCs harboring the canonical *MYB:NFIB* fusion and variable mutations including those in the *NOTCH* gene family, *BCOR, RUNX1, RIT1,* and other genes.

Our cohort of primary sinonasal AdCCs included 31/88 (35%) cases (both with canonical and noncanonical fusions) associated with growth patterns of SH and/or ASGSH. These lesions, first recognized and described by our group,[31] lack the typical lobular arrangement of SH, displaying an irregular and angled overall shape with atypical and disorganised inner secretory epithelial cells and outer myoepithelial cells. These lesions harbor both canonical *MYB*/*MYBL1:NFIB* fusions and noncanonical fusions. The possible precursor/neoplastic nature of ASGSH was supported by various mutations revealed by NGS in 5 cases, including *BRAF* Val600Glu (2 cases), *RET* Arg912Trp (2 cases), and *FAT1* Pro1665Leu (1 case).[31] According to our recent observations, ASGSH structures may also be associated with other sinonasal malignancies, such as low-grade tubulopapillary adenocarcinoma and a subset of sinonasal adenosquamous carcinoma.[33]

Sinonasal AdCCs are particularly aggressive salivary gland malignancies, mostly with poor clinical outcome and no effective systemic therapy.[8,12] Therefore, identifying potentially targetable genetic alterations in AdCC is crucial. Our findings confirm several observations from previous AdCC whole exome sequencing studies. Somatic mutations in *NOTCH1, NOTCH2* and other Notch pathway molecules have been reported previously in AdCC.[13,34–36] In our cohort, *NOTCH1* was one of the most commonly disrupted genes (in 14% of analyzable cases). Notch signaling with its pleiotropic, context-dependent effects on cell differentiation, survival, and growth is disrupted in many human malignancies.[37,38] *NOTCH1* alterations can result in either tumor suppression or oncogenesis, depending on the tumor

entity.[39,40] Further characterization of Notch signaling alterations in AdCC is warranted, particularly since it is a potentially targetable pathway.[41] Patients with such aberrations might potentially benefit from anti-NOTCH drugs, such as Brontictuzumab.[41]

Morphologically, all 3 *NOTCH*-mutated AdCCs in our series revealed a prevailing solid/basaloid pattern with a minor component of cribriform and tubular patterns. These tumors were characterized by confluent solid sheets of tumor cells with pronounced nuclear enlargement and polymorphism, and high mitotic and Ki-67 indices, along with perineural, intraneural and bone invasion, and comedonecrosis. In addition to high-grade morphology, metatypical features were noted in 2 AdCCs with *NOTCH* mutations. They presented with unusual growth patterns, including squamous differentiation, tubular epithelial hypereosinophilia with luminal cell prominence and focal sebaceous metaplasia. The clinical outcome of the 3 patients with *NOTCH*-mutated AdCCs was particularly poor.

In our study, 19 cases displayed atypical morphologic features consistent with metatypical AdCC, including tubular epithelial hypereosinophilia, vacuolated clear cells, and small clusters, cords and isolated tumor cells in hyalinized extracellular matrix.[18,19] Multiple foci of foamy vacuolated eosinophilic cells within tumor nests composed of basaloid neoplastic cells were present in 1 case. Similar groups of vacuolated neoplastic cells were previously described by Altemani et al,[30] although their tumors were not termed metatypical AdCC, as they called such cells signet-ring cells. In our study, 3 of the 5 AdCCs with metatypical morphology harbored noncanonical fusions *ESWR1:DNM3*, *EWSR1:MYB*, or *ACTN4:MYB*, while 1 had the canonical *MYB:NFIB* fusion, and in 1 case no fusion was detected. In addition, all 5 metatypical AdCCs displayed multiple mutations in genes such as *NOTCH3, PTEN, CHD2, ARID1B, RB1, APC, CSF3R, SPEN, NCOR1, KDM6A, BCOR, GATA3,* or *MET*. The clinical outcome of patients with metatypical AdCCs harboring *NOTCH* and *BCOR* gene mutations was notably poor.

The clinical significance of mutations in several of the genes identified in this study has not been previously investigated in AdCC. We found mutations in SWI/SNF complex genes, in particular in *SMARCA4, ARID1A,* and *PBRM1*. The latter is known to be required for stability of the SWI/SNF chromatin remodeling complex. The PI3K-Akt pathway was represented by the *PTEN* gene, the RAS/MAPK pathway by the *RIT1* and *NF1* genes, and the Wnt signaling pathway by the *CDH2* and *CCD1* genes. However, none of the mutations observed in this study had a high recurrence rate in our sinonasal AdCCs, and consequently they do not appear to play essential roles in the pathogenetic mechanism of AdCC. In contrast, it is likely that they have pathogenetic importance for those rare patients whose tumors harbor them.

In conclusion, this study emphasizes the significance of broad molecular profiling in expanding our understanding of AdCC. No morphologic differences were observed between AdCCs with *MYBL1:NFIB* and *MYB:NFIB* fusions. Mutations in the *NOTCH* genes were associated with high-grade and metatypical phenotypes, and worse clinical outcome. Noncanonical fusions were predominantly associated with metatypical AdCC. These discoveries illustrate how broad molecular profiling enables correlating morphologic changes, genetic alterations, and tumor behavior in AdCCs.

REFERENCES

1. WHO Classification of Tumours Editorial Board. *Head and Neck Tumours*. Lyon, France: International Agency for Research on Cancer. forthcoming (WHO classification of tumours series, 5th ed.; vol. 9) https://publications.iarc.fr
2. Persson M, Andren Y, Mark J, et al. Recurrent fusion of MYB and NFIB transcription factor genes in carcinomas of the breast and head and neck. *Proc Natl Acad Sci USA*. 2009;106:18740–18744.
3. Fujii K, Murase T, Beppu S, et al. *MYB, MYBL1, MYBL2* and *NFIB* gene alterations and MYC overexpression in salivary gland adenoid cystic carcinoma. *Histopathology*. 2017;71:823–834.
4. Persson M, Andren Y, Moskaluk CA, et al. Clinically significant copy number alterations and complex rearrangements of *MYB* and *NFIB* in head and neck adenoid cystic carcinoma. *Genes Chromosomes Cancer*. 2012;51:805–817.
5. Šteiner P, Andreasen S, Grossmann P, et al. Prognostic significance of 1p36 locus deletion in adenoid cystic carcinoma of the salivary glands. *Virchows Arch*. 2018;473:471–480.
6. Skálová A, Klubíčková N, Bradová M, et al. Discovery of novel *TULP4/ACTN4/EWSR1/ACTB::MYB* and *ESRRG::DNM3* fusions expands molecular landscape of adenoid cystic carcinoma beyond fusions between *MYB/MYBL1* and *NFIB* genes. *Am J Surg Pathol*. 2024;48:1503–1511.
7. Bjørndal K, Krogdahl A, Therkildsen MH, et al. Salivary adenoid cystic carcinoma in Denmark 1990-2005: outcome and independent prognostic factors including the benefit of radiotherapy. Results of the Danish Head and Neck Cancer Group (DAHANCA). *Oral Oncol*. 2015;51:1138–1142.
8. Mauthe T, Holzmann D, Soyka MB, et al. Overall and disease-specific survival of sinonasal adenoid cystic carcinoma: a systematic review and meta-analysis. *Rhinology*. 2023;61:508–518.
9. Suárez C, Barnes L, Silver CE, et al. Cervical lymph node metastasis in adenoid cystic carcinoma of oral cavity and oropharynx: a collective international review. *Auris Nasus Larynx*. 2016;43:477–484.
10. Kawakita D, Murase T, Ueda K, et al. The impact of clinicopathological factors on clinical outcomes in patients with salivary gland adenoid cystic carcinoma: a multi-institutional analysis in Japan. *Int J Clin Oncol*. 2020;25:1774–1785.
11. Cavalieri S, Mariani L, Vander Poorten V, et al. Prognostic nomogram in patients with metastatic adenoid cystic carcinoma of the salivary glands. *Eur J Cancer*. 2020;136:35–42.
12. Trope M, Triantafillou V, Kohanski MA, et al. Adenoid cystic carcinoma of the sinonasal tract: a review of the national cancer database. *Int Forum Allergy Rhinol*. 2019;9:427–434.
13. Ho AS, Kannan K, Roy DM, et al. The mutational landscape of adenoid cystic carcinoma. *Nat Genet*. 2013;45:791–798.
14. Ho AS, Ochoa A, Jayakumaran G, et al. Genetic hallmarks of recurrent/metastatic adenoid cystic carcinoma. *J Clin Invest*. 2019;129:4276–4289.
15. Xie M, Wei S, Wu X, et al. Alterations of Notch pathway in patients with adenoid cystic carcinoma of the trachea and its impact on survival. *Lung Cancer*. 2018;121:41–47.
16. Ferrarotto R, Heymach JV. Taking it up a NOTCH: a novel subgroup of ACC is identified. *Oncotarget*. 2017;8:81725–81726.
17. Ferrarotto R, Mitani Y, Diao L, et al. Activating NOTCH1 mutations define a distinct subgroup of patients with adenoid cystic carcinoma who have poor prognosis, propensity to bone and liver metastasis, and potential responsiveness to Notch1 inhibitors. *J Clin Oncol*. 2017;35:352–360.
18. Mathew EP, Todorovic E, Truong T, et al. Metatypical adenoid cystic carcinoma: a variant showing prominent squamous differ-

entiation with a predilection for the sinonasal tract and skull base. *Am J Surg Pathol*. 2022;46:816–822.
19. Weinreb I, Rooper LM, Dickson BC, et al. Adenoid cystic carcinoma with striking tubular hypereosinophilia: a unique pattern associated with nonparotid location and both canonical and novel *EWSR1::MYB* and *FUS::MYB* fusions. *Am J Surg Pathol*. 2023;47: 497–503.
20. Perzin KH, Gullane P, Clairmont AC. Adenoid cystic carcinomas arising in salivary glands; a correlation of histologic features and clinical course. *Cancer*. 1978;42:265–282.
21. Szanto PA, Luna MA, Tortoledo ME, et al. Histologic grading of adenoid cystic carcinoma of the salivary glands. *Cancer*. 1984;54: 1062–1069.
22. Spiro RH, Huvos AG, Strong EW. Adenoid cystic carcinoma of salivary origin. A clinicopathologic study of 242 cases. *Am J Surg*. 1974;128:512–520.
23. van Weert S, van der Waal I, Witte BI, et al. Histopathological grading of adenoid cystic carcinoma of the head and neck: analysis of currently used grading systems and proposal for a simplified grading scheme. *Oral Oncol*. 2015;51:71–76.
24. Landrum MJ, Lee JM, Benson M, et al. ClinVar: improving access to variant interpretations and supporting evidence. *Nucleic Acids Res*. 2018;46(D1):D1062–D1067.
25. Koboldt DC. Best practices for variant calling in clinical sequencing. *Genome Med*. 2020;12:91–104.
26. Michal M, Berry RS, Rubin BP, et al. *EWSR1-SMAD3*-rearranged fibroblastic tumor: an emerging entity in an increasingly more complex group of fibroblastic/myofibroblastic neoplasms. *Am J Surg Pathol*. 2018;42:1325–1333.
27. van Dongen JJ, Langerak AW, Bruggemann M, et al. Design and standardization of PCR primers and protocols for detection of clonal immunoglobulin and T-cell receptor gene recombinations in suspect lymphoproliferations: report of the BIOMED-2 Concerted Action BMH4-CT98-3936. *Leukemia*. 2003;17:2257–2317.
28. Kazakov DV, Nemcova J, Mikyskova I, et al. Human papillomavirus in lesions of anogenital mammary-like glands. *Int J Gynecol Pathol*. 2007;26:475–480.
29. Hagmar B, Johansson B, Kalantari M, et al. The incidence of HPV in a Swedish series of invasive cervical carcinoma. *Med Oncol Tumor Pharmacother*. 1992;9:113–117.
30. Altemani A, Costa AF, Montalli VA, et al. Signet-ring cell change in adenoid cystic carcinoma: a clinicopathological and immunohistochemical study of four cases. *Histopathology*. 2013;62: 531–542.
31. Michal M, Skálová A, Hyrcza M, et al. Nasal and sinonasal tumors formed by atypical adenomatous lesions arising in respiratory epithelial adenomatoid hamartoma/seromucinous hamartoma. *Virchows Arch*. 2024;485:31–42.
32. Mitani Y, Rao PH, Futreal PA, et al. Novel chromosomal rearrangements and break points at the t(6;9) in salivary adenoid cystic carcinoma: association with *MYB-NFIB* chimeric fusion, MYB expression, and clinical outcome. *Clin Cancer Res*. 2011;17: 7003–7014.
33. Bradova M Costes-Martineau V Laco J et alet al. Sinonasal adenosquamous carcinomas arising in seromucinous hamartoma or respiratory epithelial adenomatoid hamartoma with atypical features: report of 5 detailed clinicopathologic and molecular characterization of rare entity. *Histopathology*. 2024. doi: 10.1111/his.15369. Epub ahead of print..
34. Stephens PJ, Davies HR, Mitani Y, et al. Whole exome sequencing of adenoid cystic carcinoma. *J Clin Invest*. 2013;123:2965–2968.
35. Ross JS, Wang K, Rand JV, et al. Comprehensive genomic profiling of relapsed and metastatic adenoid cystic carcinomas by next-generation sequencing reveals potential new routes to targeted therapies. *Am J Surg Pathol*. 2014;38:235–238.
36. Aster JC, Blacklow SC. Targeting the Notch pathway: twists and turns on the road to rational therapeutics. *J Clin Oncol*. 2012;30: 2418–2420.
37. Agrawal N, Frederick MJ, Pickering CR, et al. Exome sequencing of head and neck squamous cell carcinoma reveals inactivating mutations in *NOTCH1*. *Science*. 2011;333:1154–1157.
38. Rettig EM, Chung CH, Bishop JA, et al. Cleaved NOTCH1 expression pattern in head and neck squamous cell carcinoma is associated with NOTCH1 mutation, HPV status, and high-risk features. *Cancer Prev Res (Phila)*. 2015;8:287–295.
39. Ranganathan P, Weaver KL, Capobianco AJ. Notch signalling in solid tumours: a little bit of everything but not all the time. *Nat Rev Cancer*. 2011;11:338–351.
40. Kagawa S, Natsuizaka M, Whelan KA, et al. Cellular senescence checkpoint function determines differential Notch1-dependent oncogenic and tumor-suppressor activities. *Oncogene*. 2015;34:2347–2359.
41. Miller LE, Au V, Mokhtari TE, et al. A contemporary review of molecular therapeutic targets for adenoid cystic carcinoma. *Cancers (Basel)*. 2022;14:992.